Charge dynamics in molecular junctions: Nonequilibrium Green's function approach made fast

S. Latini,[1] E. Perfetto,[1] A.-M. Uimonen,[2] R. van Leeuwen,[2,3] and G. Stefanucci[1,3,4]

[1]*Dipartimento di Fisica, Università di Roma Tor Vergata, Via della Ricerca Scientifica 1, 00133 Rome, Italy*

[2]*Department of Physics, Nanoscience Center, FIN 40014, University of Jyväskylä, Jyväskylä, Finland*

[3]*European Theoretical Spectroscopy Facility (ETSF)*

[4]*INFN, Laboratori Nazionali di Frascati, Via E. Fermi 40, 00044 Frascati, Italy*

(Received 19 November 2013; revised manuscript received 10 January 2014; published 11 February 2014)

Real-time Green's function simulations of molecular junctions (open quantum systems) are typically performed by solving the Kadanoff-Baym equations (KBE). The KBE, however, impose a serious limitation on the maximum propagation time due to the large memory storage needed. In this work we propose a simplified Green's function approach based on the generalized Kadanoff-Baym ansatz (GKBA) to overcome the KBE limitation on time, significantly speed up the calculations, and yet stay close to the KBE results. This is achieved through a twofold advance: First, we show how to make the GKBA work in open systems and then construct a suitable quasiparticle propagator that includes correlation effects in a diagrammatic fashion. We also provide evidence that our GKBA scheme, although already in good agreement with the KBE approach, can be further improved without increasing the computational cost.

DOI: 10.1103/PhysRevB.89.075306 PACS number(s): 05.60.Gg, 05.10.−a, 73.63.−b, 72.10.Bg

I. INTRODUCTION

Charge transfer through nanoscale interfaces is a ubiquitous dynamical process in molecular electronics, photovoltaics, electroluminiscence, and transient spectroscopy, to mention a few emerging fields of research [1,2]. The complexity of the molecules (or molecular aggregate) and of the contacts to a source/drain electrode, as well as the simultaneous interplay of Coulomb repulsion and vibrational effects make these research fields an interdisciplinary topic where physics, chemistry, and engineering meet. Reliable theoretical predictions require an accurate description of the nuclear degrees of freedom, a careful selection of the electronic basis functions, and a proper treatment of correlation effects.

Among the *ab initio* methods, density functional theory [3,4] (DFT) and its time-dependent extension [5,6] (TDDFT) stand out for the advantageous scaling of the computational cost with increasing the system size and the propagation time. However, as for any other method, a (TD)DFT implementation is based on some approximation and, at present, the available approximations are inadequate to capture correlation effects like the Coulomb blockade [7–9] or the polarization-induced renormalization of the molecular levels [10–14]. These effects are particularly important in a donor-acceptor complex, in a molecular junction in the weak-coupling regime and more generally when the transition rate for an electron to move from one atom to another is small. Many-body approaches based on nonequilibrium Green's functions [15–18] (NEGF) offer a promising alternative as the relevant scattering processes to describe the aforementioned effects can be incorporated either through a proper selection of Feynman diagrams or through a decoupling scheme for the higher order Green's functions. Real-time simulations within the NEGF are performed by solving the Kadanoff-Baym equations [15,19–21] (KBE), which are a set of coupled nonlinear integrodifferential equations for the one-particle Green's function. Unfortunately, the price to pay in solving the KBE is that the computational time scales cubically with the propagation time (given the self-energy), whereas in TDDFT the scaling is linear (given the exchange-correlation potential).

In the mid-1980s Lipavsky *et al.*[22] proposed an approximation to scale down the computational time (from cubic to quadratic) of the KBE. This approximation is known as the generalized Kadanoff-Baym ansatz (GKBA) and has been successfully applied to strongly interacting nuclear matter [23]; electron plasma [24,25]; carrier dynamics of semiconductors [8,26–31]; optical absorption spectra [32]; quasiparticle spectra [33]; and, more recently, excited Hubbard clusters [34–36]. In all these cases the system is either a bulk periodic system or a finite system. It is currently unknown how the GKBA performs for nanostructures chemically bonded to or adsorbed on a surface (open system). In fact, in open systems a number of issues have to be addressed before a GKBA calculation can be carried out. For instance the GKBA remains an approximation even in a noninteracting (or mean-field) treatment, whereas in closed systems it is exact. Furthermore the performance of the GKBA strongly depends on the quality of the quasiparticle propagator and, as we shall see, in open systems the available approximations perform rather poorly.

This work contains a thorough study of the GKBA in open systems. In Sec. II we derive the fundamental equations and present a few exact properties. Here the discussion is mainly focussed on noninteracting and mean-field electrons. Important aspects of the GKBA like the construction of a mean-field propagator as well as issues related to relaxation and local thermalization are analyzed and addressed. This preliminary investigation is particularly relevant since, as previously mentioned, the GKBA is an approximation already at the mean-field level. In the correlated case the GKBA simulations using a mean-field propagator are far off the KBE results. In Sec. III we propose a couple of correlated propagators to remedy this deficiency. Our propagators have the merit of scaling quadratically with the propagation time and, hence, the computational gain of the GKBA is maintained. The different GKBA schemes are compared with the full KBE approach in Sec. IV. We consider two systems, a molecular junction under applied bias and a donor-acceptor complex under illumination, and calculate local currents and densities. Both systems constitute a severe test for the GKBA as the

inclusion of correlations changes dramatically the mean-field picture. The important message emerging from this study is that one of the proposed GKBA schemes is in fairly, sometimes extremely, good agreement with the KBE approach. We also provide numerical evidence that the GKBA scheme can be further improved at the same computational cost. In conclusion, time-dependent simulations of open systems within the NEGF framework can be made much faster.

II. GKBA IN OPEN SYSTEMS

In this section we briefly review the KBE for open systems and discuss in detail the simplifications brought about by the GKBA. The most general Hamiltonian which describes a molecular junction in contact with M electronic reservoirs has the form

$$\hat{H} = \sum_{\alpha=1}^{M} \hat{H}_\alpha + \hat{H}_J + \hat{H}_T. \tag{1}$$

In Eq. (1) the Hamiltonian of the α reservoir reads

$$\hat{H}_\alpha = \sum_{k\alpha\sigma} \epsilon_{k\alpha} \hat{d}^\dagger_{k\alpha\sigma} \hat{d}_{k\alpha\sigma} \tag{2}$$

with $\hat{d}_{k\alpha\sigma}$ the annihilation operator for electrons of spin σ and energy $\epsilon_{k\alpha}$. The Hamiltonian of the molecular junction is expressed in terms of the operators $\hat{d}_{i\sigma}$ for electrons of spin σ in the i-th localized molecular orbital,

$$\hat{H}_J = \sum_{\substack{ij\\ \sigma}} h_{ij} \hat{d}^\dagger_{i\sigma} \hat{d}_{j\sigma} + \frac{1}{2} \sum_{\substack{ijmn\\ \sigma\sigma'}} v_{ijmn} \hat{d}^\dagger_{i\sigma} \hat{d}^\dagger_{j\sigma'} \hat{d}_{m\sigma'} \hat{d}_{n\sigma}, \tag{3}$$

where h_{ij} are the one-electron matrix elements of the one-body part (kinetic plus potential energy) and v_{ijmn} are the two-electron Coulomb integrals. The last term in Eq. (1) is the tunneling Hamiltonian between the different subsystems and reads

$$\hat{H}_T = \sum_{k\alpha\sigma} \sum_i (T_{k\alpha,i} \hat{d}^\dagger_{k\alpha\sigma} \hat{d}_{i\sigma} + \text{H.c.}) \tag{4}$$

with $T_{k\alpha,i}$ the tunneling amplitude between the i-th state of the molecular junction and the k state of the α reservoir.

Initially, say at time $t = 0$, the system is in equilibrium at inverse temperature β and chemical potential μ. We assume that this equilibrium state can be reached starting from the uncontacted ($T_{k\alpha,i} = 0$) and noninteracting ($v_{ijmn} = 0$) system in the remote past, $t = -\infty$, and then propagating forward in time with the full interacting and contacted Hamiltonian until $t = 0$. This amounts to assume that initial-correlation and memory effects are washed out. In our experience this assumption is always verified [37,38]. At time $t = 0$ the system is driven out of equilibrium by external electromagnetic fields, $\epsilon_{k\alpha} \to \epsilon_{k\alpha} + V_\alpha(t)$ and $h_{ij} \to h_{ij}(t)$. We are interested in monitoring the evolution of the electronic degrees of freedom through the calculation of observable quantities like, e.g., the local occupation and current.

A. Green's function and KBE

The building block of any diagrammatic many-body approach is the Green's function defined according to [15]

$$G_{ij}(z,z') = \frac{1}{i} \langle \mathcal{T}\{\hat{d}_{i\sigma,H}(z) \hat{d}^\dagger_{j\sigma,H}(z')\}\rangle. \tag{5}$$

In this definition the symbol "$\langle\cdots\rangle$" denotes a grand-canonical average, and $\mathcal{T}$ is the contour ordering acting on operators in the Heisenberg picture. The Green's function has arguments z and z' on the contour γ going from $-\infty$ to ∞ (forward branch) and back from ∞ to $-\infty$ (backward branch). On this contour G_{ij} satisfies the equations of motion [39] (in matrix form)

$$\left[i\frac{d}{dz} - h_{\text{HF}}(z) \right] G(z,z') = \delta(z,z') + \int_\gamma d\bar{z}\, \Sigma(z,\bar{z}) G(\bar{z},z') \tag{6}$$

and its adjoint. Let us describe the various quantities in this equation. The Hartree-Fock (HF) single-particle Hamiltonian is the sum of h and the HF potential

$$h_{\text{HF},ij} = h_{ij} + \sum_{mn} (2v_{imnj}\rho_{nm} - v_{imjn}\rho_{nm}), \tag{7}$$

where

$$\rho_{nm}(z) \equiv -iG_{nm}(z,z^+) \tag{8}$$

is the time-dependent single-particle density matrix. The kernel $\Sigma = \Sigma_{\text{em}} + \Sigma_c$ is the sum of the so-called embedding self-energy and the correlation self-energy. The former can be calculated directly from the parameters of the Hamiltonian and reads

$$\Sigma_{\text{em},ij}(z,z') = \sum_{k\alpha} T_{i,k\alpha} g_{k\alpha}(z,z') T_{k\alpha,j}, \tag{9}$$

where

$$g_{k\alpha}(z,z') = \frac{1}{i}[\theta(z,z')\bar{f}(\epsilon_{k\alpha}) - \theta(z',z) f(\epsilon_{k\alpha})] e^{-i\phi_{k\alpha}(z,z')} \tag{10}$$

is the Green's function of the disconnected α reservoir. In Eq. (10) $f(\epsilon) = 1/(e^{\beta(\epsilon-\mu)}+1)$ is the Fermi function, $\bar{f}(\epsilon) = 1 - f(\epsilon)$, and the phase $\phi_{k\alpha}(z,z') = \int_{z'}^{z} d\bar{z}(\epsilon_{k\alpha} + V_\alpha(\bar{z}))$. The expression of the correlation self-energy depends on the choice of diagrams that we decide to include. In this work we consider the second Born (2B) approximation, which has been shown to produce results very close to those of the GW approximation [37] and to those of numerically exact techniques in model systems [40]. The 2B approximation has the merit of capturing two important correlation effects in molecular transport, namely the renormalization and broadening of the quasiparticle levels. Of course, the 2B approximation is not adequate to describe more strongly correlated effects like the Coulomb blockade or the Kondo effect. In these cases one could generate Σ_c from, e.g., decoupling schemes like those described in Ref. [41].

The 2B self-energy is given by the sum of the lowest-order bubble diagram plus the second-order exchange diagram, see

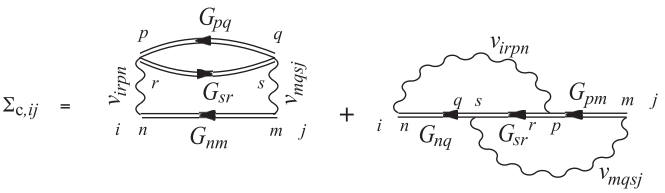

FIG. 1. Diagrams for the 2B correlation self-energy.

Fig. 1 [42],

$$\Sigma_{c,ij}(z,z') = \sum_{nmpqrs} v_{irpn} v_{mqsj} [2G_{nm}(z,z')G_{pq}(z,z')G_{sr}(z',z) - G_{nq}(z,z')G_{sr}(z',z)G_{pm}(z,z')]. \quad (11)$$

To solve Eq. (6) we convert it into a set of coupled equations, known as the KBE, for real-time (as opposed to contour-time) quantities. This is done by letting z vary on the forward (backward) branch and z' vary on the backward (forward) branch of the contour γ. Using the Langreth rules [15,43] to convert contour-time convolutions into real-time convolutions, we find (in matrix form)

$$\left[i\frac{d}{dt} - h_{\rm HF}(t) \right] G^<(t,t') = I^<(t,t') \quad (12)$$

$$G^>(t,t') \left[-i\frac{\overleftarrow{d}}{dt'} - h_{\rm HF}(t') \right] = I^>(t,t') \quad (13)$$

with collision integrals

$$I^<(t,t') = \int_{-\infty}^{\infty} d\bar{t} [\Sigma^<(t,\bar{t})G^A(\bar{t},t') + \Sigma^R(t,\bar{t})G^<(\bar{t},t')], \quad (14)$$

$$I^>(t,t') = \int_{-\infty}^{\infty} d\bar{t} [G^>(t,\bar{t})\Sigma^A(\bar{t},t') + G^R(t,\bar{t})\Sigma^>(\bar{t},t')]. \quad (15)$$

Here the superscripts "$>$, $<$, R, A" refer to the lesser, greater, retarded, and advanced Keldysh components. Equations (12) and (13) are solved by use of a time-stepping technique, starting from a value $G^{\lessgtr}(t_{\rm in},t_{\rm in})$ at some initial time $t_{\rm in} < 0$ and then evolving along the directions t and t' until a maximum propagation time $t_{\rm max}$. The time $t_{\rm in}$ is chosen remotely enough in the past in order to have full relaxation at $t = 0$, time at which the external fields are switched on [44]. As $I^{\lessgtr}(t,t')$ in Eqs. (14) and (15) involves integrals between $t_{\rm in}$ (the self-energy vanishes for times smaller than $t_{\rm in}$ since the system is initially uncontacted and noninteracting) and either t or t', the numerical effort in solving the KBE scales like $t_{\rm max}^3$.

B. GKBA

The GKBA allows us to reduce drastically the computational time. The basic idea consists in obtaining a closed equation for the equal time $G^<$ from which to calculate the time-dependent averages of all one-body observables like, e.g., density, current, dipole moment, and so on. The GKBA is therefore an ansatz for the density matrix [45] $\rho(t) = -iG^<(t,t)$, not for the spectral function which has to be approximated separately (see below).

The exact equation for $\rho(t)$ follows from the difference between Eq. (12) and its adjoint and reads

$$\frac{d}{dt}\rho(t) + i[h_{\rm HF}(t),\rho(t)] = -(I^<(t,t) + {\rm H.c.}). \quad (16)$$

This is not a closed equation for ρ as the collision integral contains the off-diagonal (in time) $G^{\lessgtr}$. To close Eq. (16) we make the GKBA [22]

$$G^<(t,t') = iG^R(t,t')G^<(t',t') - iG^<(t,t)G^A(t,t') = -G^R(t,t')\rho(t') + \rho(t)G^{\rm A}(t,t') \quad (17)$$

and, similarly,

$$G^>(t,t') = G^R(t,t')\bar{\rho}(t') - \bar{\rho}(t)G^A(t,t'), \quad (18)$$

where $\bar{\rho}(t) = 1 - \rho(t) = iG^>(t,t)$. However, the GKBA alone is not enough to close Eq. (16) since the quasiparticle propagator G^R (and, hence, $G^A = [G^R]^\dagger$), or, equivalently, the spectral function, remains unspecified. The possibility of using the GKBA in open systems strongly relies on the choice of G^R. This is an important point which we thoroughly address in the next section. For the time being we observe that the numerical effort in solving Eq. (16) scales like $t_{\rm max}^2$ provided that the calculation of G^R does not scale faster [46].

1. Exact properties

Among the properties of the GKBA we mention the fulfillment of the relation $G^R - G^A = G^> - G^<$ for any choice of G^R and the fact that Eqs. (17) and (18) become an identity in the limit $t \to t'$ since $G^R(t^+,t) = -i$. Another valuable feature (in systems out of equilibrium) is that the GKBA preserves the continuity equation. There is, however, an even more important property from which the physical contents of the GKBA become evident. In closed systems ($\Sigma_{\rm em} = 0$) and for HF electrons ($\Sigma_c = 0$) the collision integrals vanish and Eqs. (17) and (18) are the solution of Eqs. (12) and (13) provided that G^R is the HF propagator [8,15],

$$G^R(t,t') = -i\theta(t-t')\,T\,e^{-i\int_{t'}^{t} d\bar{t}\, h_{\rm HF}(\bar{t})}, \quad (19)$$

where T is the time-ordering operator. Therefore, the more the quasiparticle picture is valid the more the GKBA is accurate. A more exhaustive discussion on the range of applicability of the GKBA in closed systems can be found in Refs. [22,47,48].

In open systems the GKBA is not the solution of the HF equations since $\Sigma_{\rm em} \neq 0$ and, hence, the collision integral is nonvanishing. The reliability of the GKBA in open systems needs to be investigated already at the HF level. In HF the collision integrals are evaluated with $\Sigma = \Sigma_{\rm em}$ and G^R being the solution of

$$\left[i\frac{d}{dt} - h_{\rm HF}(t) \right] G^R(t,t') = \delta(t,t') + \int d\bar{t}\, \Sigma^R_{\rm em}(t,\bar{t})G^R(\bar{t},t'). \quad (20)$$

In HF-GKBA the collision integrals are evaluated with $\Sigma = \Sigma_{\rm em}$, $G^<(\bar{t},t') = \rho(\bar{t})G^{\rm A}(\bar{t},t')$, and $G^A = [G^R]^\dagger$ some suitable propagator. If we calculate G^R from Eq. (20), then the numerical advantage of the GKBA is lost since the

computational cost of solving this equation scales like $t_{\max}^3$. Thus the questions are as follows: Can a "computationally cheap" propagator be constructed for open systems? If so, how accurate is the solution of the HF-GKBA equation?

To answer these questions, we consider a wide-band-limit (WBL) embedding self-energy $\Sigma^R_{\rm em}(t,t') = -(i/2)\Gamma\delta(t-t')$, where Γ is a positive-semidefinite self-adjoint matrix. In this case the solution of Eq. (20) is

$$G^R(t,t') = -i\theta(t-t')\,T\,e^{-i\int_{t'}^{t} d\bar{t}\,(h_{\rm HF}(\bar{t})-i\Gamma/2)}, \qquad (21)$$

which has the same mathematical structure of Eq. (19). In particular, it has the group property

$$G^R(t+\delta,t') = iG^R(t+\delta,t)G^R(t,t') \qquad (22)$$

and, hence, the number of operations to calculate G^R for all $t < t_{\max}$ and $t' < t$ scales like $t_{\max}^2$. The HF collision integral reads

$$I^<(t,t) = \int_{-\infty}^{\infty} d\bar{t}\,\Sigma^<_{\rm em}(t,\bar{t})G^A(\bar{t},t) - \frac{i}{2}\Gamma G^<(t,t), \qquad (23)$$

whereas the HF-GKBA collision integral reads

$$I^<(t,t) = \int_{-\infty}^{\infty} d\bar{t}\,\Sigma^<_{\rm em}(t,\bar{t})G^A(\bar{t},t) - \frac{i}{2}\Gamma\rho(t)G^A(t^-,t). \qquad (24)$$

If in Eq. (24) we use for $G^A = [G^R]^\dagger$ the HF result in Eq. (21), then the collision integrals are identical since $G^A(t^-,t) = i$ and $i\rho(t) = G^<(t,t)$. We conclude that the $G^<(t,t)$ that solves the HF and HF-GKBA equations is the *same* provided that we use the same G^R of Eq. (21). This observation contains useful hints on how to approximate the quasiparticle propagator of open systems without paying a too-high computational price. We emphasize that the locality in time of the retarded embedding self-energy and of the HF self-energy $\Sigma_{\rm HF}(z,z') = \delta(z,z')[h_{\rm HF}(z) - h(z)]$ are distinct and should not be lumped together. The former is purely imaginary and, hence, $\Sigma^<_{\rm em} \neq 0$, whereas the latter is purely real and, hence, $\Sigma^<_{\rm HF} = 0$. Alternatively, we can say that $\Sigma_{\rm HF}$ is local on the contour, whereas $\Sigma_{\rm em}$ is not. This is a crucial difference: In closed systems the off-diagonal HF-GKBA $G^<(t,t')$ is the same as the HF $G^<(t,t')$, whereas in open systems it remains an approximation even for a WBL embedding self-energy. Only the diagonal HF and HF-GKBA $G^<(t,t)$ are identical in this case.

2. *An approximate propagator for mean-field electrons*

In most physical situations the removal and addition energies relevant to describe the electron dynamics of the molecular junction after the application of a voltage difference or a laser pulse are well inside the continuum spectrum of the reservoirs. It is therefore natural to study how well the GKBA equation performs when G^R is chosen as in Eq. (21) with

$$\Gamma = i\left[\Sigma^R_{\rm em}(\mu) - \Sigma^A_{\rm em}(\mu)\right]. \qquad (25)$$

In Eq. (25) the quantity $\Sigma^R_{\rm em}(\mu)$ is the Fourier transform of the equilibrium embedding self-energy evaluated at the chemical potential. This choice of Γ is expected to yield accurate results whenever $\Sigma^R_{\rm em}(\omega)$ depends weakly on ω for frequencies around μ. Let us address this issue numerically. We consider a class of systems consisting of two reservoirs, $\alpha = L,R$,

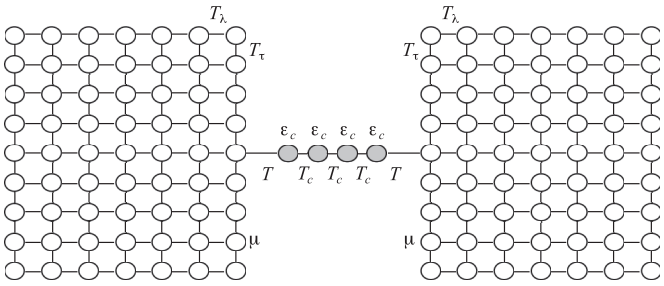

FIG. 2. Example of an open system as described in the main text with $N_\tau = 9$ transverse channels and a chain of four sites.

with N_τ transverse channels and a nanostructure with a chain geometry; see Fig. 2. We use a tight-binding representation and characterize the Hamiltonian of the reservoirs by a transverse hopping T_τ and a longitudinal hopping T_λ between nearest-neighboring sites and an onsite energy $\epsilon = \mu$ (half-filled reservoirs). The molecular chain has matrix elements $h_{ij} = T_c$ between nearest-neighboring sites i and j and $h_{ii} = \epsilon_c$ on the diagonal. The left reservoir is contacted through its middle terminal site to the leftmost site of the chain while the right reservoir is contacted through its middle terminal site to the rightmost site of the chain. We denote by T the corresponding matrix elements of the Hamiltonian [49].

In Fig. 3 we compare GKBA versus full KBE results for noninteracting and HF electrons. In all cases the Coulomb integrals $v_{ijmn} = \delta_{in}\delta_{jm}v_{ij}$. The top panels refer to a system with $N_\tau = 1$ and a single-site chain driven out of equilibrium

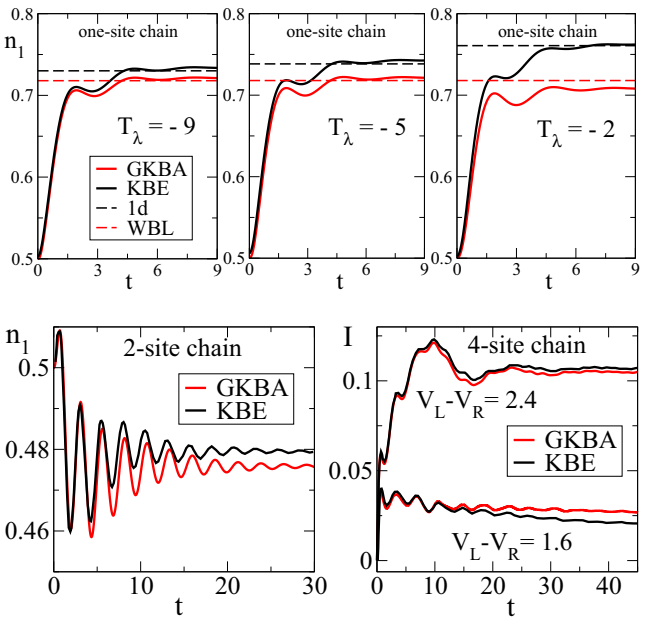

FIG. 3. (Color online) Top panels: Density $n_1 = \rho_{11}$ of a one-site chain connected to leads with $N_\tau = 1$ after the sudden switch-on of a bias $V_L = 2$ for different $T_\lambda = -9, -5, -2$. Bottom left panel: HF density of site 1 of a two-site chain connected to leads with $N_\tau = 1$ after the sudden switch-on of a bias $V_L = -V_R = 1$. Bottom right panel: HF current at the right interface of a four-site chain connected to leads with $N_\tau = 9$ after the sudden switch-on of a bias $V_L = -V_R = 0.8, 1.2$.

by a bias $V_L = 2$ and $V_R = 0$. The parameters (in arbitrary units) are $\mu = \epsilon_c = 0$, $v_{ij} = 0$, and $T = \sqrt{\gamma|T_\lambda|/2}$ with $\gamma = 0.4$. From Eq. (25) we find $\Gamma = 2\gamma$. The simulations have been performed at zero temperature for three different values of $T_\lambda = -9, -5, -2$, and are compared with exact numerical results obtained using the algorithm of Ref. [50]. As expected the agreement deteriorates with decreasing the bandwidth $W = 4|T_\lambda|$ of the reservoirs since $\Sigma^R_{\rm em}(\omega)$ acquires a strong dependence on ω for ω in the bias window. The dashed lines indicate the steady-state value of n_1 for one-dimensional reservoirs and for WBL reservoirs. KBE correctly approaches the one-dimensional steady state in all cases, whereas GKBA approaches the WBL steady state only in the limit $|T_\lambda| \to \infty$. In the bottom left panel we consider a two-site chain driven out of equilibrium by a bias $V_L = -V_R = 1$ and again connected to one-dimensional reservoirs [37]. In this case, however, the system is interacting and treated in the HF approximation. The chemical potential is chosen in the middle of the highest occupied molecular orbital–lowest unoccupied molecular orbital (HOMO-LUMO) gap of the disconnected chain with two electrons. For $T_c = -1$, $\epsilon_c = 0$, and Coulomb integrals $v_{11} = v_{22} = 2, v_{12} = v_{21} = 1$ one finds $\mu = 2$. The rest of the parameters are $T_\lambda = -1.5$ and $T = -0.5$ which, from Eq. (25), implies $\Gamma \simeq 0.67$ for the GKBA simulations. Even though the HOMO-LUMO gap $\Delta_{\rm HL} = 2$ is not much smaller than the bandwidth $W = 4|T_\lambda| = 6$, we still observe a satisfactory agreement for the density of site 1 (a similar agreement is found for site 2, not shown). The damping time as well as the amplitude and frequency of the transient oscillations are well reproduced; furthermore, the GKBA steady-state value differs by less than 1% from the corresponding KBE value. The accuracy of the HF-GKBA is not limited to the diagonal matrix elements of the density matrix. This is exemplified in the bottom right panel, where we show the current flowing at the right interface of the four-site chain of Fig. 2 with $N_\tau = 9$ transverse channels, bias $V_L = -V_R = 0.8, 1.2$, chemical potential $\mu = 2.26$ (chosen in the middle of the HOMO-LUMO gap of the disconnected chain with 4 electrons), $T_c = -1, T_\lambda = T_\tau = -2, T = -0.5, \epsilon_c = 0$, and Coulomb integrals $v_{ii} = v = 1.5$ and $v_{ij} = (v/2)/|i - j|$ for $i \neq j$ [39]. The GKBA and KBE currents are in excellent agreement except for a slight overestimation of the GKBA steady-state value at small bias.

In conclusion, the GKBA equation with G^R from Eq. (21) and Γ from Eq. (25) is a good approximation to study the HF dynamics of open systems provided that the embedding self-energy of the reservoirs has a weak frequency dependence around the chemical potential.

3. Relaxation and local thermalization

For the GKBA results of Fig. 3 we started the propagation at time $t_{\rm in} < 0$ with the HF density matrix of the uncontacted system and let $\rho(t)$ thermalize in the absence of external fields until $t = 0$ when a bias is switched on. For $t_{\rm in}$ sufficiently remote in the past the density matrix attains a steady value $\rho_{\rm eq}$ before the system is biased. By definition $\rho_{\rm eq}$ is the static solution of Eq. (16) with $d\rho/dt = 0$; therefore if we start with $\rho(t_{\rm in}) = \rho_{\rm eq}$, then the density matrix remains constant in the interval $(t_{\rm in},0)$. In the left panel of Fig. 4 we plot

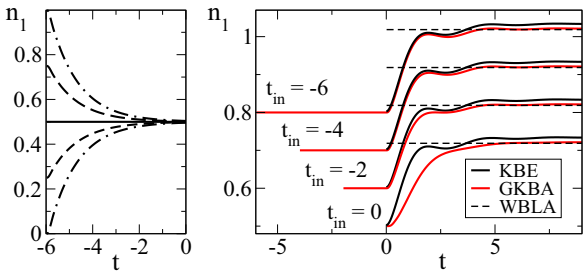

FIG. 4. (Color online) Results for the density $n_1(t)$ of the one-site chain with $T_\lambda = -9$ and same parameters as in Fig. 3. In the left panel the system is unperturbed and $n_1(t_{\rm in})$ is varied. In the right panel $n_1(t_{\rm in}) = 1/2$, a bias $V_L = 2$ is switched on at $t = 0$ and $t_{\rm in}$ is varied. For clarity the curves with $t_{\rm in} = -2n, n = 0,1,2,3$ are shifted upward by $n/10$.

the time-dependent density of the noninteracting one-site chain of Fig. 3 for different initial values; we see that $n_1(t) = \rho_{11}(t) = 1/2$ for all $t < 0$ if $n_1(t_{\rm in} = -6) = 1/2$ is the thermalized value. It is tempting to reduce the computational time (provided that one finds a simpler way to determine $\rho_{\rm eq}$) by starting the propagation at $t = 0$ with $\rho(0) = \rho_{\rm eq}$. This initial condition guarantees the local thermalization of all one-time observables. However, in a fully relaxed system any two-time correlator depends on the time difference only, and to achieve this relaxation a "memory buffer" is needed. Suppose that we start the propagation with $G^<(t_{\rm in},t_{\rm in}) = i\rho_{\rm eq}$. Then the equal-time $G^<(t,t)$ remains constant but the $G^<(t,t')$ depends on t and t' separately. It is only for large-enough t,t' that $G^<(t,t')$ depends on $t - t'$. This concept is explained in the right panel of Fig. 4, where we display $n_1(t)$ when a bias $V_L = 2$ is switched on at $t = 0$. In all cases $\rho(t_{\rm in}) = \rho_{\rm eq} = 1/2$ but the initial time $t_{\rm in}$ is varied. The absence of relaxation for too small $|t_{\rm in}|$ is evident from the strong dependence of the transient behavior on $t_{\rm in}$. The curves $n_1(t > 0)$ become independent of $t_{\rm in}$ only for $t_{\rm in} \lesssim -4$.

The concept of relaxation, and, hence, of the memory buffer, has been illustrated in a simple model system but its importance is completely general and is not limited to systems in thermal equilibrium. Suppose that the physical system is in some excited state $\rho_{\rm ex}$. If we start the propagation at time $t = 0$ with initial condition $\rho(0) = \rho_{\rm ex}$, then the transient behavior is affected by spurious relaxation processes. The proper way of performing GKBA simulations consists in driving the relaxed system toward $\rho_{\rm ex}$ with some suitable external fields.

4. Damping

For bulk systems like an electron gas the inclusion of damping in the propagator worsens the agreement with the KBE results [25]. In fact, the use of a non-Hermitian quasiparticle Hamiltonian $h_{\rm HF} - i\Gamma/2$ in G^R is a distinctive feature of open systems. Here we address how sensitive the results are to different values of Γ. We consider again the noninteracting one-site chain of Fig. 3 with $T_\lambda = -9$, for which Eq. (25) yields $\Gamma = 0.8$. In all cases we set the initial condition $n_1(t_{\rm in}) = 1$. In Fig. 5 (left panel) we show the relaxation dynamics, starting from $t_{\rm in} = -8$, of the unperturbed system for three different Γ; the curves are essentially on top of each other. This may

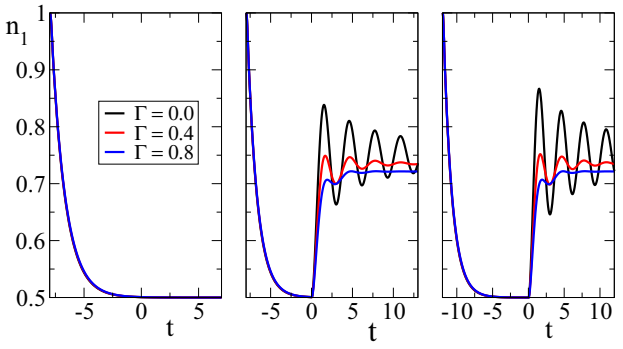

FIG. 5. (Color online) Time-dependent occupation of the one-site chain for different Γ. Left panel: $t_{\rm in} = -8$ and unperturbed system. Middle panel: $t_{\rm in} = -8$ and bias $V_L = 2$ switched on at $t = 0$. Right panel: $t_{\rm in} = -12$ and bias $V_L = 2$ switched on at $t = 0$.

suggest that the dependence on Γ is weak. However, if we switch on a bias in the left lead $V_L = 2$ at time $t = 0$ (middle panel) we appreciate a strong Γ dependence. We may argue that for small Γ the relaxation time is longer and, hence, that the curves with $\Gamma = 0.0,\ 0.4$ approach the curve with $\Gamma = 0.8$ by reducing $t_{\rm in}$. This is not the case as clearly illustrated in the right panel, where $t_{\rm in} = -12$. The curve with $\Gamma = 0.4$ is already converged, whereas the one with $\Gamma = 0$ is not but the trend is to separate further from the curve with $\Gamma = 0.8$. The apparent weak Γ dependence in the left panel is simply due to the alignment of the on-site energy to the chemical potential, $\mu = \epsilon_c = 0$. In general a proper choice of the quasiparticle damping is crucial for a correct description of the system evolution. In HF theory the damping is only due to embedding effects and the Γ of Eq. (25) is the most accurate. The inclusion of correlation effects introduces an extra damping. Is it possible to maintain the simple form in Eq. (21) for the quasiparticle propagator and still have good agreement with the KBE results? In the next section we discuss two different correlated quasiparticle Hamiltonians to insert in Eq. (21).

III. CORRELATED APPROXIMATIONS TO THE PROPAGATOR

In the interacting case the exact equation of motion for $G^{\rm R}$ reads

$$\left[i\frac{d}{dt} - h_{\rm HF}(t)\right]G^R(t,t') = \delta(t,t') + \int d\bar{t}\,\Sigma^R(t,\bar{t})G^R(\bar{t},t') \tag{26}$$

with $\Sigma^R = \Sigma^R_{\rm em} + \Sigma^R_c$. If we approximate

$$\Sigma^R_{\rm em}(t,t') \simeq -(i/2)\Gamma\delta(t-t'), \tag{27}$$

with Γ from Eq. (25), we find the approximate equation

$$\left[i\frac{d}{dt} - h^{(0)}_{\rm qp}(t)\right]G^R(t,t') = \delta(t,t') + \int d\bar{t}\,\Sigma^R_c(t,\bar{t})G^R(\bar{t},t'), \tag{28}$$

where

$$h^{(0)}_{\rm qp}(t) \equiv h_{\rm HF}(t) - i\Gamma/2 \tag{29}$$

is the HF quasiparticle Hamiltonian. Discarding the integral on the right-hand side of Eq. (28), one finds the HF solution of Eq. (21). We refer to the GKBA with HF propagators as the GKBA0 scheme. Unfortunately the GKBA0 scheme performs rather poorly, see Sec. IV, indicating that G^R has to incorporate correlation effects to some extent. Below we propose two schemes to approximate the convolution $\Sigma^R G^R$ and reduce Eq. (28) to a quasiparticle equation of the form

$$\left[i\frac{d}{dt} - h_{\rm qp}(t)\right]G^R(t,t') = \delta(t,t'). \tag{30}$$

The solution of Eq. (30) is

$$G^R(t,t') = -i\theta(t-t')\,T\,e^{-i\int_{t'}^{t} d\bar{t}\,h_{\rm qp}(\bar{t})} \tag{31}$$

and satisfies the group property of Eq. (22). Therefore, if we are successful in this task the calculation of G^R will scale like $t^2_{\rm max}$.

A. Static correlation approximation

In open systems the correlation self-energy decays to zero when the separation between its time arguments approaches infinity. If $G^R(\bar{t},t') \simeq G^R(t,t')$ for $t - \bar{t}$ smaller than the decay time of Σ^R_c we can approximately write

$$\int d\bar{t}\,\Sigma^R_c(t,\bar{t})G^R(\bar{t},t') \simeq \left[\int d\bar{t}\,\Sigma^R_c(t,\bar{t})\right]G^R(t,t'). \tag{32}$$

To evaluate the integral in the square brackets we make an adiabatic approximation on top of the GKBA, i.e., we replace G^R with the equilibrium propagator of a system described by the Hamiltonian $\hat{H}(t)$. Let us consider, for simplicity, an interaction $v_{ijmn} = \delta_{in}\delta_{jm}v_{ij}$. Then the Langreth rules [15,43] provides us with the following expression of the retarded 2B self-energy [see Eq. (11)]:

$$\begin{aligned}
\Sigma^R_{c,ij}&(t,t') \\
&= 2\sum_{kl} v_{ik}v_{jl}\big[G^R_{ij}(t,t')G^<_{lk}(t',t)G^>_{kl}(t,t') \\
&\quad + G^<_{ij}(t,t')G^A_{lk}(t',t)G^<_{kl}(t,t') + G^<_{ij}(t,t')G^<_{lk}(t',t)G^R_{kl}(t,t')\big] \\
&\quad - \sum_{kl} v_{ik}v_{jl}\big[G^R_{il}(t,t')G^<_{lk}(t',t)G^>_{kj}(t,t') \\
&\quad + G^<_{il}(t,t')G^A_{lk}(t',t)G^<_{kj}(t,t') + G^<_{il}(t,t')G^<_{lk}(t',t)G^R_{kj}(t,t')\big].
\end{aligned} \tag{33}$$

As $\Sigma^R_c(t,t')$ vanishes for $t < t'$, the GKBA transforms this quantity into a function of $\rho(t)$ and $G^R(t,t') = [G^A(t',t)]^\dagger$. The adiabatic approximation consists in evaluating the GKBA form of Eq. (33) using an equilibrium propagator

$$\tilde{G}^R(t,t-t') = \int \frac{d\omega}{2\pi}\frac{e^{-i\omega(t-t')}}{\omega - h_{\rm qp}(t) + i\eta}, \tag{34}$$

where we use the matrix notation $1/A = A^{-1}$ for any matrix A. The resulting expression, which we denote by $\tilde{\Sigma}(t,t-t')$, depends implicitly on t through the dependence on $\rho(t)$ and $h_{\rm qp}(t)$ and explicitly on $t - t'$. If we define

$$\tilde{\Sigma}(t) = \int d\bar{t}\,\tilde{\Sigma}(t,t-\bar{t}), \tag{35}$$

then the right-hand side of Eq. (32) becomes $\tilde{\Sigma}(t)G^R(t,t')$ and Eq. (28) is solved by Eq. (31) with

$$h_{\rm qp}(t) = h_{\rm HF}(t) - i\Gamma/2 + \tilde{\Sigma}(t). \tag{36}$$

In this way we generate a self-consistent equation for $\tilde{\Sigma}(t) = \tilde{\Sigma}(\rho(t),h_{\rm qp}(t))$. In practice, for a given $\tilde{\Sigma}(t_n)$ at the n-th time step we determine $\rho(t_{n+1})$ from Eq. (16), then calculate $h_{\rm qp}(t_{n+1}) = h_{\rm HF}(t_{n+1}) - i\Gamma/2 + \tilde{\Sigma}(t_n)$, hence, $\tilde{G}^R(t_{n+1},t_{n+1}-t')$, and, finally, $\tilde{\Sigma}(t_{n+1})$. Each time step can be repeated a few times to achieve convergence; in our experience two predictor correctors are typically enough. It is worth stressing that the propagator appearing in the collision integral is G^R and not $\tilde{G}^R$. The latter is only an auxiliary quantity to calculate $\tilde{\Sigma}(t)$. In the following we refer to the combination of GKBA with the described propagator as the GKBA+static correlation (SC) scheme since Eq. (35) is the zero frequency value of the Fourier transform of $\tilde{\Sigma}(t,t-\bar{t})$. In this scheme the calculation of $\tilde{\Sigma}$ for a given $\tilde{G}^R$ scales like N^5, where N is the number of basis functions in the molecular junction.

B. Quasiparticle approximation

An alternative way to introduce correlation effects in the propagator is again based on the adiabatic approximation but uses the concept of quasiparticles. Let us represent operators in the one-particle Hilbert space with a hat, e.g., $\hat{h}_{\rm qp}$ or $\hat{\Sigma}^R_c$, and denote by $|i\rangle$ the basis ket of the molecular junction so $\langle i|\hat{\Sigma}^R_c|j\rangle = \hat{\Sigma}^R_{c,ij}$, and so on. For an isolated molecule in equilibrium the quasiparticle equation reads

$$\left[\hat{h}_{\rm HF} + \hat{\Sigma}^R_c(\epsilon)\right]|\varphi\rangle = \epsilon|\varphi\rangle, \tag{37}$$

where $\hat{\Sigma}^R_c(\epsilon)$ is the Fourier transform of the equilibrium self-energy. To lowest order in Σ^R_c this equation implies that the correction to the HF energies $\epsilon_{{\rm HF},n}$ is

$$\epsilon_{{\rm qp},n} = \epsilon_{{\rm HF},n} + \langle\varphi_n|\hat{\Sigma}^R_c(\epsilon_{{\rm HF},n})|\varphi_n\rangle, \tag{38}$$

where $|\varphi_n\rangle$ is the eigenket of $\hat{h}_{\rm HF}$ with eigenvalue $\epsilon_{{\rm HF},n}$. Equation (38) suggests constructing a quasiparticle Hamiltonian in the following manner. We evaluate again the GKBA form of Eq. (33) with the propagator of Eq. (34) and then calculate

$$\tilde{\Sigma}(t,\omega) = \int dt\, e^{i\omega(t-t')}\tilde{\Sigma}(t,t-t'). \tag{39}$$

From this quantity we construct the one-particle operator $\hat{\tilde{\Sigma}}(t,\omega) = \sum_{ij}|i\rangle\tilde{\Sigma}_{ij}(t,\omega)\langle j|$ and subsequently the diagonal self-energy operator in the HF basis,

$$\hat{\tilde{\Sigma}}(t) = \sum_n |\varphi_n\rangle\langle\varphi_n|\hat{\tilde{\Sigma}}(t,\epsilon_{{\rm HF},n})|\varphi_n\rangle\langle\varphi_n|. \tag{40}$$

Imposing now that $\hat{h}_{\rm qp}(t) = \hat{h}^{(0)}_{\rm qp}(t) + \hat{\tilde{\Sigma}}(t)$ we get a self-consistent equation for $\tilde{\Sigma}(t)$. We refer to this procedure as the GKBA+quasiparticle (QP) scheme. As the Fourier transform of $\tilde{\Sigma}(t,t-t')$ has to be evaluated in N different energies, the calculation of $\tilde{\Sigma}(t)$ in the GKBA+QP scheme scales like N^6.

IV. RESULTS

In this section we study the nonequilibrium *correlated* dynamics of the chain junction of Fig. 2 and of a model photovoltaic junction. We calculate local occupations, currents, and spectral functions using different GKBA schemes and benchmark the results against full KBE simulations. A clear-cut scenario will emerge in which GKBA + SC is the most reliable scheme while all other schemes suffer from some deficiencies.

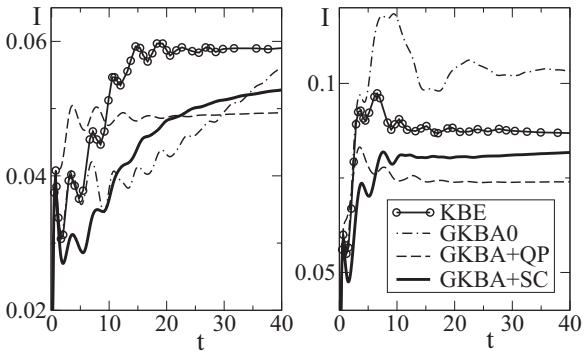

FIG. 6. Time-dependent current at the right interface of the four-site junction with $V_L - V_R = 1.6$ (left panel) and 2.4 (right panel); same parameters as in Fig. 4.

A. Chain junction

Nonequilibrium correlation effects change drastically the HF picture of quantum transport. The applied bias causes an enhancement of quasiparticle scatterings and, consequently, a substantial broadening of the spectral peaks [39,51]. The 2B steady current is larger (smaller) than the HF steady current at bias smaller (larger) than the HF HOMO-LUMO gap, see bottom-right panel of Fig. 4. In Fig. 6 we compare the current at small (left panel) and large (right panel) bias using KBE and different GKBA schemes. Even though the correlation-induced enhancement (at small bias $V_L - V_R = 1.6$ the HF steady current is $\sim$0.023) and suppression (at large bias $V_L - V_R = 2.4$ the HF steady current is $\sim$0.11) of the steady current relative to the HF values is qualitatively captured by all GKBA schemes, quantitative differences emerge. GKBA0 is rather close to KBE during the initial transient but considerably overestimates the steady state. GKBA+QP corrects this deficiency too much and the steady current is appreciably underestimated. Furthermore, the transient behavior worsens: The first peak is absent and the current saturates too fast. This is due to a general problem of the GKBA+QP scheme. The equilibrium $\tilde{\Sigma}$ is too large or, equivalently, equilibrium correlations are overestimated. GKBA + SC gives an overall improvement. The transient current reproduces several KBE features (oscillation frequency and relative hight of the peaks) and the steady current is very close to the KBE value.

By construction the GKBA schemes guarantee the satisfaction of the continuity equation. The rate of change of the total number of electrons in the nanostructure, dN/dt, is equal to the sum of the currents flowing through the left and right interface, $I_L + I_R$. In Fig. 7 we show that this analytic property is numerically confirmed with high accuracy in the GKBA+QP and GKBA + SC schemes.

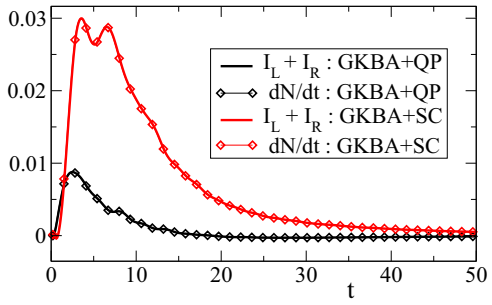

FIG. 7. (Color online) Numerical evidence of the fulfillment of the continuity equation in the GKBA+QP and GKBA + SC schemes.

B. Photovoltaic junction

We consider a more complicated open system with the features of a photovoltaic molecular junction. Inspired by a paper by Li *et al.* [52], we model the junction as a donor-acceptor complex connected to left and right electrodes (reservoirs); see Fig. 8. The donor is described by HOMO (h) and LUMO (l) levels and the LUMO is connected to a chain of four acceptor sites each described by a single localized orbital. These orbitals are mixed by the acceptor Hamiltonian and form two valence and two conduction levels. The junction is connected to the left electrode throught the HOMO with tunneling amplitude $T_{L,h}$ and to the right electrode through the rightmost acceptor site with tunneling amplitude $T_{4,R}$. The explicit form of the Hamiltonian of the donor-acceptor complex is

$$\begin{aligned}\hat{H}_J &= \epsilon_h \hat{n}_h + \epsilon_l \hat{n}_l + \epsilon_A \sum_{a=1}^{4} \hat{n}_a + T_{\rm DA} \sum_{\sigma} (\hat{d}^\dagger_{l\sigma} \hat{d}_{1\sigma} + \hat{d}^\dagger_{1\sigma} \hat{d}_{l\sigma}) \\ &+ T_A \sum_{a=1}^{3} \sum_{\sigma} (\hat{d}^\dagger_{a\sigma} \hat{d}_{a+1\sigma} + \hat{d}^\dagger_{a+1\sigma} \hat{d}_{a\sigma}) \\ &+ U_{\rm DA}(\hat{n}_h + \hat{n}_l - 2) \sum_{a=1}^{4} \frac{\hat{n}_a - 1}{a}, \end{aligned} \tag{41}$$

where $\hat{n}_x = \sum_\sigma \hat{d}^\dagger_{x\sigma} \hat{d}_{x\sigma}$ is the occupation operator for $x = h,l,a$. The interaction between the excess charges of the donor and acceptor chain implicitly fixes the condition of charge neutrality. For one-dimensional reservoirs with longitudinal hopping integral $T_\lambda = -9$, tunneling amplitudes $T_{L,h} = T_{4,R} = -0.3$, donor levels $\epsilon_h = -2.92$, $\epsilon_l = -0.92$, acceptor levels $\epsilon_A = -2.08$, donor-acceptor hopping $T_{\rm DA} = -0.1$, intra-acceptor hopping $T_A = -0.2$, and interaction $U_{\rm DA} = 0.5$, the chemical potential $\mu = 0.04$ is in the middle

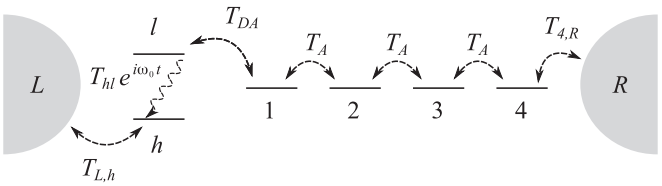

FIG. 8. Schematic illustration of the photovoltaic junction described in the main text.

of the HF gap between the valence and conduction acceptor levels. The equilibrium system has HOMO and LUMO occupations 2 and 0, respectively, and the two valence levels of the acceptor chain completely filled. The photovoltaic junction is driven out of equilibrium by irradiation with monochromatic light. For simplicity we assume that the light couples only to the donor dipole moment and, hence,

$$\hat{H}_{\rm light}(t) = s(t) T_{hl} \sum_{\sigma} (e^{i\omega_0 t} \hat{d}^\dagger_{h\sigma} \hat{d}_{l\sigma} + e^{-i\omega_0 t} \hat{d}^\dagger_{l\sigma} \hat{d}_{h\sigma}), \tag{42}$$

where $s(t)$ is a switching function. We consider $T_{hl} = 0.3$, $\omega_0 = 2 = |\epsilon_h - \epsilon_l|$, and study a pulse, $s(t) = 1$, for $0 < t < \pi/T_{hl}$ and zero otherwise, as well as continuous radiation, $s(t) = 1$ for $t > 0$ and $s(t) = 0$ for $t < 0$.

In order to apply many body perturbation theory we need to rewrite $\hat{H}_J$ in the form of Eq. (3). The last term of Eq. (41) contains quadratic terms $\hat{d}^\dagger \hat{d}$ as well as quartic terms of the form $\hat{d}^\dagger \hat{d} \hat{d}^\dagger \hat{d}$ (density-density) instead of $\hat{d}^\dagger \hat{d}^\dagger \hat{d} \hat{d}$, see Eq. (3). To extract the Coulomb integrals v_{ijmn} to be used in the 2B self-energy we simply use the anticommutation rules and then group all the quadratic terms to construct the one-particle Hamiltonian h_{ij}. The latter, with indices $i,j = h,l,a$, reads

$$h = \begin{pmatrix} \tilde{\epsilon}_h & 0 & 0 & 0 & 0 & 0 \\ 0 & \tilde{\epsilon}_l & T_{DA} & 0 & 0 & 0 \\ 0 & T_{DA} & \tilde{\epsilon}_{A\,1} & T_A & 0 & 0 \\ 0 & 0 & T_A & \tilde{\epsilon}_{A\,2} & T_A & 0 \\ 0 & 0 & 0 & T_A & \tilde{\epsilon}_{A\,3} & T_A \\ 0 & 0 & 0 & 0 & T_A & \tilde{\epsilon}_{A\,4} \end{pmatrix}, \tag{43}$$

with $\tilde{\epsilon}_h = \epsilon_h + \frac{25}{12} U_{\rm DA}$, $\tilde{\epsilon}_l = \epsilon_l + \frac{25}{12} U_{\rm DA}$, and $\tilde{\epsilon}_{A\,a} = \epsilon_A + \frac{25}{6} U_{\rm DA} - 2\, U_{\rm DA}/a$. For the Coulomb integrals we find $v_{ijmn} = \delta_{in}\delta_{jm} v_{ij}$ with

$$v = U_{\rm DA} \begin{pmatrix} 0 & 0 & 1 & 1/2 & 1/3 & 1/4 \\ 0 & 0 & 1 & 1/2 & 1/3 & 1/4 \\ 1 & 1 & 0 & 0 & 0 & 0 \\ 1/2 & 1/2 & 0 & 0 & 0 & 0 \\ 1/3 & 1/3 & 0 & 0 & 0 & 0 \\ 1/4 & 1/4 & 0 & 0 & 0 & 0 \end{pmatrix}. \tag{44}$$

Let us start with the mean-field analysis of the light pulse. The duration π/T_{hl} has been chosen to get a population inversion of the HOMO and LUMO levels. In Fig. 9 we show the HF occupations of the donor (top panel) and acceptor (bottom panel) levels in GKBA and KBE. The impressive agreement is due to the fact that for $T_\lambda = -9$ the WBL approximation is extremely good. The depletion of charge on the first acceptor site (A1) is a consequence of the repulsive interaction $U_{\rm DA}$. During the pulse the HOMO level is partially refilled by the left reservoir and the total charge on the donor overcomes 2. This excess charge is instantaneously felt by A1 which starts expelling electrons at a rate larger than the tunneling rate from LUMO to A1. We also observe that the charge transfer between LUMO and A1 is not effective. The inset shows the LUMO occupation on a longer time scale. Electrons remain trapped and slosh around along the junction. In fact, in HF no steady state is reached. The occurrence of self-sustained charge oscillations in mean-field treatments has been observed in similar contexts [14,53] and is most likely an artifact of the approximation. As we shall see,

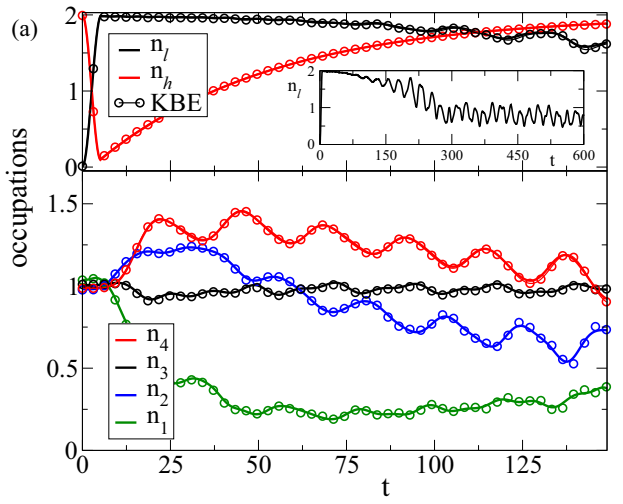

FIG. 9. (Color online) Time-dependent occupations in the HF approximation using GKBA (solid) and KBE (circles). The junction is perturbed by a monochromatic pulse.

the correlated KBE results differ substantially. Therefore the collision integral and the correlated propagator of the GKBA approach have to correct the HF theory in a substantial manner.

With the inclusion of correlations a deficiency of the GKBA+QP scheme emerges already during the thermalization process. In Fig. 10 the donor and acceptor occupations are propagated within different schemes in the absence of external fields using the HF value of the uncontacted system and $\tilde{\Sigma}(t_{\rm in}) = 0$ as initial conditions. Both GKBA0 and GKBA + SC thermalize, similarly to HF, to values very close to the equilibrium values of the correlated (2B) KBE approach (dotted horizontal line). In fact, in KBE the HF and 2B equilibrium occupations are essentially the same since the correlation self-energy, except for a slight renormalization of the quasiparticle energies (image charge effect), does not affect the width of the spectral peaks. For the GKBA to reproduce the KBE thermalized values the imaginary part of $\tilde{\Sigma}$ has

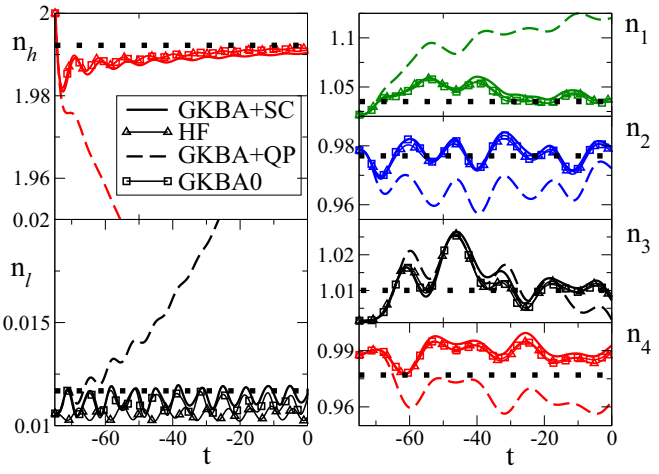

FIG. 10. (Color online) Thermalization of the occupations in the correlated case. The correlated KBE value is represented by a dotted horizontal line.

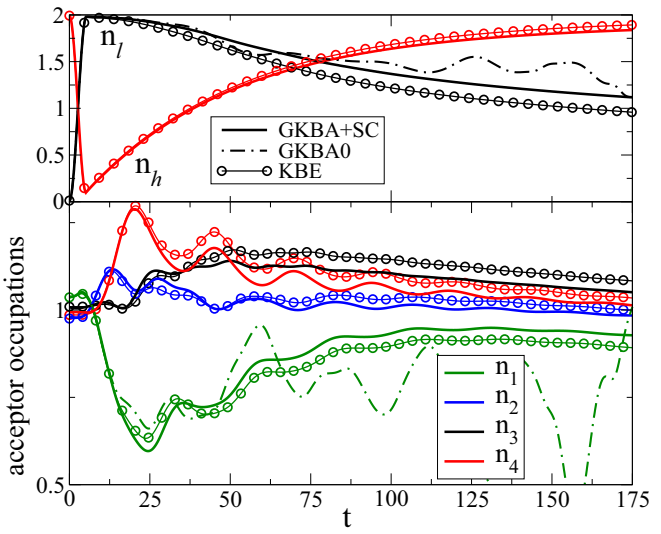

FIG. 11. (Color online) Time-dependent occupations after a pulse in KBE and GKBA + SC. For n_l and n_1 we also show the results of the GKBA0 scheme (dotted-dashed).

to be small, and this is not the case in GKBA+QP. Here $\mathrm{Im}[\tilde{\Sigma}_{ll}(t)]$ and $\mathrm{Im}[\tilde{\Sigma}_{hh}(t)]$ tend to increase thus broadening the HOMO and LUMO spectral peaks. Hence, the HOMO looses charge, whereas the LUMO acquires charge and the donor polarizability increases. This makes the first bubble diagram of the 2B self-energy larger and therefore the HOMO and LUMO spectral peaks more broadened. In a separate calculation (not shown) we simulated the GKBA+QP thermalization and found that the thermalization process is extremely slow, $t_{\rm in} \lesssim -1000$, and that the thermalized value of, e.g., the LUMO occupation is $\sim$0.7, well above the KBE result.

We are now ready to show the correlated results in the case of a light pulse. The KBE occupations are shown in Fig. 11 and considerably differ from the HF occupations of Fig. 9. The GKBA + SC scheme is in fairly good agreement with KBE *for all* occupations. To illustrate the crucial role played by our correlated propagator we also display the LUMO and A1 occupations in the GKBA0 scheme (dotted-dashed line). Even though the initial transient is acceptable the GKBA0 occupations soon become inaccurate. Therefore the evaluation of the GKBA collision integral with HF propagator performs rather poorly in open systems. The GKBA + SC scheme has the merit of working both in and out of equilibrium.

Like the only goal of TDDFT is to reproduce the density of an interacting system, so the only goal of the GKBA is to reproduce the density matrix of an interacting system. The TDDFT or GKBA spectral function $A(t,t') = i[G^R(t,t') - G^A(t,t')]$ can differ substantially from the true one. This is, however, not always the case. In Fig. 12 we show the time evolution of the KBE and GKBA + SC total spectral function defined according to

$$A(T,\omega) = -2\mathrm{Im}\int d\tau e^{i\omega\tau}\mathrm{Tr}\left[G^R\left(T+\frac{\tau}{2},T-\frac{\tau}{2}\right)\right], \quad (45)$$

where $T = (t+t')/2$ is the center-of-mass time and $\tau = t - t'$ is the relative time. Remarkably, the two spectral functions have several common features. The most important one is the

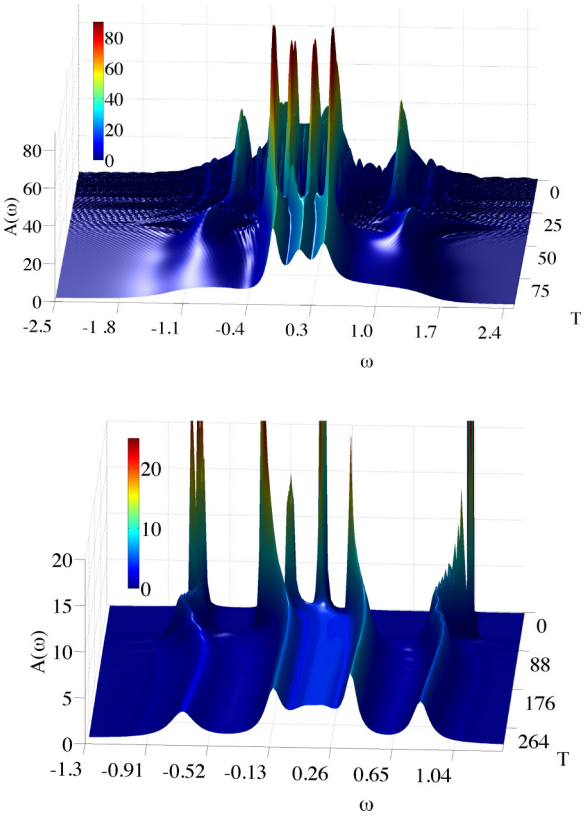

FIG. 12. (Color online) Time-dependent KBE (top panel) and GKBA + SC (bottom panel) spectral functions for the photovoltaic junction subject to a light pulse. The light pulse is switched on at time $t = 40$ for the KBE and $t = 75$ for the GKBA + SC. The parameters are the same as in Fig. 11.

broadening of the spectral peaks after the pulse and the long elapsing time to relax back to the equilibrium state. Another common feature is the drift of the acceptor peaks toward higher energy and the merging of the two middle peaks of the acceptor chain. In GKBA0 the spectral peaks are sharp at all times, whereas in GKBA+QP they are broadened at all times (not shown). The fact that the GKBA + SC spectral function resembles the KBE spectral function is probably due to the fact that the driving frequency is small enough. In fact, the underlying SC framework is based on slow-enough time variations on the electronic time scale.

To end our discussion on the performance of GKBA in open systems we consider in Fig. 13 the occupations for the continuous radiation. Here GKBA + SC is not as accurate as in the case of the light pulse. However, the agreement with KBE remains satisfactory. The HOMO and LUMO occupations are essentially indistinguishable from the KBE values (top panel). The occupations of the acceptor sites next to the right electrode (A3 and A4) are slightly underestimated in GKBA + SC but the overall trend (transient oscillations and steady-state value) are correctly reproduced (middle panel). A more quantitative agreement is observed for the acceptor sites next to the donor (A1 and A2). For the A1 occupation we also show the GKBA0 occupation (bottom panel) and we note again that after a short time the result deviates considerably from the KBE result.

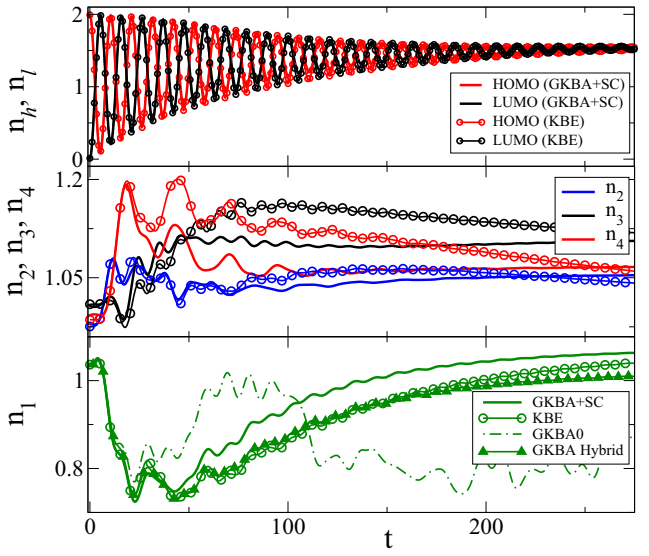

FIG. 13. (Color online) Time-dependent occupations in the presence of continuous radiation in KBE and GKBA + SC. For n_1 we also show the results of the GKBA0 scheme as well as of the hybrid scheme (thermalization with GKBA + SC, positive-time propagation with GKBA+QP).

Is there any possibility of improving the GKBA + SC scheme using a different $\tilde{\Sigma}$ or is the only way to go beyond the GKBA? In the bottom panel of Fig. 13 we display the A1 occupations for a hybrid scheme in which $\tilde{\Sigma}$ is calculated from GKBA + SC at negative times (thermalization) and from GKBA+QP at positive times. The improvement up to times $t \sim 200$ is impressive and extend to *all* acceptor occupations (not shown). Instead, for times $t > 200$ the KBE results are closer to those of the GKBA + SC scheme. More generally, for $t \lesssim 200$ we observed that the hybrid scheme performs better than GKBA + SC for $\omega_0 \sim \epsilon_h - \epsilon_l$ (large current in the junction) and worse otherwise (small current in the junction). The purpose of this investigation is to provide numerical evidence of the existence of a $\tilde{\Sigma}$ for accurate GKBA simulations and, hence, the possibility of improving the GKBA + SC scheme without increasing the computational cost.

V. SUMMARY AND OUTLOOK

We demonstrated that time-dependent NEGF simulations of molecular junctions (and, more generally, open quantum systems) can be considerably speeded up. Different GKBA-based schemes have been proposed and subsequently benchmarked against full KBE calculations. The GKBA + SC scheme turned out to be the most accurate both in and out of equilibrium, while still offering a significant computational gain (for the longest propagation ($t_{\max} = 300$) of the photovoltaic junction the CPU time is ∼10 min in GKBA + SC and ∼20 h in KBE). We also showed that the GKBA + SC scheme can, in principle, be further improved without rising the computational price.

All calculations have been performed within the 2B approximation for the correlation self-energy but the GKBA + SC scheme is completely general and not limited to this special

case. Clearly, in large nanostructures screening is important and the interaction should be treated, at least, within the GW approximation. Another urgent extension of the GKBA + SC scheme is the inclusion of the interaction between electrons and nuclei. This can be done either at the level of the Ehrenfest approximation [54,55] or by adding diagrams with electron-phonon vertices to the correlation self-energy [31].

The GKBA is an ansatz for the single-particle Green's function and it is designed to simplify the calculation of the TD average of one-body operators. The generalization of the scheme to two-body or higher-order operators would be extremely valuable, and one could assess the validity of the scheme by benchmarking the results against numerically exact data in model systems [56,57].

An important aspect of the GKBA + SC scheme (including its extensions and refinements) is that it can be implemented in *ab initio* molecular codes [58] to perform first-principles time-dependent simulations of open nanostructures. Foreseeable applications are, e.g., in the field of molecular photovoltaics and molecular electronics. Here there is much interest in developing efficient quantum simulation methods for an accurate description of the electron-hole formation, recombination, and separation as well as of charge transfer and possibly ionic reorganization or isomerization. In molecular photovoltaics *ab initio* studies have focused on the optical spectra using linear response TDDFT [59] or the Bethe-Salpeter equation [60]. Real-time simulations remain, however, the most powerful tool to resolve the different competing processes up to the ps time scale. State-of-the-art simulations treat the contacts as finite-size clusters while taking into account the full atomistic structure either semiempirically [61] or fully *ab initio* [62,63]. However, these studies suffer from spurious boundary effects like the formation of artificial electric fields and reflection of charge after a few tens of femtoseconds. There are no such limitations in the GKBA for open systems as the electrodes are described in a virtually exact way through the embedding self-energy. Furthermore, the effects of the Coulomb interaction can be systematically included through the diagrammatic expansion of the correlation self-energy. The encouraging results presented in this work should foster advances in the development of a NEGF approach to ultrafast processes at the nanoscale.

ACKNOWLEDGEMENTS

E.P. and G.S. acknowledge funding by MIUR FIRB Grant No. RBFR12SW0J and financial support through travel grants Psi-K2 5813 of the European Science Foundation (ESF). R.L. and A.U. acknowledge support from the Academy of Finland as well as the CSC IT center for providing resources for scientific computing.

[1] X.-Y. Zhu, J. Phys. Chem. B **108**, 8778 (2004).
[2] A. Nitzan, *Chemical Dynamics in Condensed Phases* (Oxford University Press, Oxford, 2006).
[3] R. M. Dreizler and E. K. U. Gross, *Density Functional Theory: An Approach to the Quantum Many-Body Problem* (Springer-Verlag, Berlin, 1990).
[4] R. G. Parr and W. Yang, *Density-Functional Theory of Atoms and Molecules* (Oxford University Press, New York, 1989).
[5] *Time-Dependent Density Functional Theory*, edited by M. A. L. Marques, C. A. Ullrich, F. Nogueira, A. Rubio, K. Burke, and E. K. U. Gross (Springer, Berlin, 2006).
[6] C. A. Ullrich, *Time-Dependent Density-Functional Theory: Concepts and Applications* (Oxford University Press, Oxford, 2012).
[7] See, e.g., *Single Charge Tunneling: Coulomb Blockade Phenomena in Nanostructures*, edited by H. Grabert and M. H. Devoret, NATO ASI Series: B, Physics, Vol. 234 (New York, Plenum Press, 1992).
[8] H. Haug and A.-P. Jauho, *Quantum Kinetics in Transport and Optics of Semiconductors* (Springer, Berlin, 2007).
[9] J. C. Cuevas and E. Scheer, *Molecular Electronics: An Introduction to Theory and Experiments* (World Scientific, Singapore, 2010).
[10] J. B. Neaton, M. S. Hybertsen, and S. G. Louie, Phys. Rev. Lett. **97**, 216405 (2006).
[11] K. Kaasbjerg and K. Flensberg, Nano Lett. **8**, 3809 (2008).
[12] K. S. Thygesen and A. Rubio, Phys. Rev. Lett. **102**, 046802 (2009).
[13] J. M. Garcia-Lastra, C. Rostgaard, A. Rubio, and K. S. Thygesen, Phys. Rev. B **80**, 245427 (2009).
[14] P. Myöhänen, R. Tuovinen, T. Korhonen, G. Stefanucci, and R. van Leeuwen, Phys. Rev. B **85**, 075105 (2012).
[15] G. Stefanucci and R. van Leeuwen, *Nonequilibrium Many-Body Theory of Quantum Systems: A Modern Introduction* (Cambridge University Press, Cambridge, 2013).
[16] P. Danielewicz, Ann. Phys. **152**, 239 (1984).
[17] R. van Leeuwen, N. E. Dahlen, G. Stefanucci, C.-O. Almbladh, and U. von Barth, Lect. Notes Phys. **706**, 33 (2006).
[18] K. Balzer and M. Bonitz, *Nonequilibrium Green's Functions Approach to Inhomogeneous Systems*, Lecture Notes in Physics (Springer-Verlag, Berlin Heidelberg, 2013), Vol. 867.
[19] L. P. Kadanoff and G. Baym, *Quantum Statistical Mechanics* (Westview Press, Boulder, CO, 1994).
[20] N.-H. Kwong and M. Bonitz, Phys. Rev. Lett. **84**, 1768 (2000).
[21] N. E. Dahlen and R. van Leeuwen, Phys. Rev. Lett. **98**, 153004 (2007).
[22] P. Lipavský, V. Špička and B. Velický, Phys. Rev. B **34**, 6933 (1986).
[23] H. S. Köhler, Phys. Rev. E **53**, 3145 (1996).
[24] M. Bonitz, D. Kremp, D. C. Scott, R. Binder, W. D. Kraeft, and H. S. Köhler, J. Phys.: Condens. Matter **8**, 6057 (1996).
[25] M. Bonitz, D. Semkat, and H. Haug, Eur. Phys. J. B **9**, 309 (1999).
[26] H. Haug, Phys. Status Solidi B **173**, 139 (1992).
[27] R. Binder, H. S. Köhler, M. Bonitz, and N. H. Kwong, Phys. Rev. B **55**, 5110 (1997).
[28] N. H. Kwong, M. Bonitz, R. Binder, and H. S. Köhler, Phys. Status Solidi B **206**, 197 (1998).
[29] P. Gartner, L. Bányai, and H. Haug, Phys. Rev. B **60**, 14234 (1999).
[30] Q. T. Vu and H. Haug, Phys. Rev. B **62**, 7179 (2000).

[31] A. Marini, J. Phys: Conf. Proc. **427**, 012003 (2013).
[32] G. Pal, Y. Pavlyukh, W. Hübner, and H. C. Schneider, Eur. Phys. J. B **79**, 327 (2011).
[33] G. Pal, Y. Pavlyukh, W. Hübner, and H. C. Schneider, Eur. Phys. J. B **70**, 483 (2009).
[34] D. Hochstuhl and M. Bonitz, J. Phys: Conf. Proc. **427**, 012007 (2013).
[35] K. Balzer, S. Hermanns, and M. Bonitz, J. Phys: Conf. Proc. **427**, 012006 (2013).
[36] M. Bonitz, S. Hermanns, and K. Balzer, Contrib. Plasma Phys. **53**, 778 (2013).
[37] P. Myöhänen, A. Stan, G. Stefanucci, and R. van Leeuwen, Europhys. Lett. **84**, 67001 (2008).
[38] Initial correlations can survive in low-dimensional and interacting reservoirs, see E. Perfetto, G. Stefanucci, and M. Cini, Phys. Rev. Lett. **105**, 156802 (2010).
[39] P. Myöhänen, A. Stan, G. Stefanucci, and R. van Leeuwen, Phys. Rev. B **80**, 115107 (2009).
[40] A.-M. Uimonen, E. Khosravi, A. Stan, G. Stefanucci, S. Kurth, R. van Leeuwen, and E. K. U. Gross, Phys. Rev. B **84**, 115103 (2011).
[41] Z. Feng, Q. Sun, L. Wan and Hong Guo, J. Phys.: Condens. Matter **23**, 415301 (2011).
[42] The second Born self-energy in Eq. (11) with all four-index two-electron integrals has been calculated in Ref. [21].
[43] D. C. Langreth, in *Linear and Nonlinear Electron Transport in Solids*, edited by J. T. Devreese and E. van Doren (Plenum, New York, 1976), pp. 3–32.
[44] Alternatively, one could add a vertical track (imaginary Matsubara axis) to the contour and starts the real-time propagation at $t = 0$; see O. V. Konstantinov and V. I. Perel's, Sov. Phys. JETP **12**, 142 (1961) as well as Ref. [16].
[45] A thorough discussion on the relation between the GKBA and density matrix theory can be found in M. Bonitz, *Quantum Kinetic Theory* (Teubner, Stuttgart-Leipzig, 1998).
[46] The GKBA is an ansatz for the lesser (greater) Green's function. At present there exists no extension of the GKBA to the left (right) Green's functions [15] for the inclusion of initial correlations through the addition of a vertical track (imaginary Matsubara axis). Therefore, relaxation can only be achieved by propagating the unperturbed (interacting and contacted) system from $t_{\rm in} < 0$ to time $t = 0$. In closed systems, due to the absence of the damping induced by the contacts, one is forced to switch the interaction on adiabatically for otherwise the system does not relax; see S. Hermanns, K. Balzer, and M. Bonitz, Phys. Scr. T **151**, 014035 (2012).
[47] B. Velický, A. Kalvová and V. Špička, J. Phys: Conf. Proc. **35**, 1 (2006).
[48] M. Bonitz and D. Kremp, Phys. Lett. A **212**, 83 (1996).
[49] For the calculation of $\Sigma_{\rm em}$ in these geometries see, e.g., Ref. [39] and S. Sanvito, C. J. Lambert, J. H. Jefferson, and A. M. Bratkovsky, Phys. Rev. B **59**, 11936 (1999).
[50] S. Kurth, G. Stefanucci, C.-O. Almbladh, A. Rubio, and E. K. U. Gross, Phys. Rev. B **72**, 035308 (2005).
[51] K. S. Thygesen, Phys. Rev. Lett. **100**, 166804 (2008).
[52] G. Li, A. Nitzan, and M. A. Ratner, Phys. Chem. Chem. Phys. **14**, 14270 (2012).
[53] E. Khosravi, A.-M. Uimonen, A. Stan, G. Stefanucci, S. Kurth, R. van Leeuwen, and E. K. U. Gross, Phys. Rev. B **85**, 075103 (2012).
[54] C. Verdozzi, G. Stefanucci, and C.-O. Almbladh, Phys. Rev. Lett. **97**, 046603 (2006).
[55] C. A. Rozzi *et al*., Nat. Commun. **4**, 1602 (2013).
[56] F. Heidrich-Meisner, A. E. Feiguin, and E. Dagotto, Phys. Rev. B **79**, 235336 (2009).
[57] C. A. Büsser and F. Heidrich-Meisner, Phys. Rev. Lett. **111**, 246807 (2013).
[58] For progresses in this direction see, e.g., A. Marini, C. Hogan, M. Grüning, and D. Varsano, Comput. Phys. Commun. **180**, 1392 (2009).
[59] F. de Angelis, S. Fantacci, and A. Selloni, Nanotechnology **19**, 424002 (2008).
[60] X. Blase, C. Attaccalite, and V. Olevano, Phys. Rev. B **83**, 115103 (2011).
[61] See, e.g., L. G. C. Rego and V. S. Batista, J. Am. Chem. Soc. **125**, 7989 (2003).
[62] W. R. Duncan, W. M. Stier, and O. V. Prezhdo, J. Am. Chem. Soc. **127**, 7941 (2005).
[63] W. R. Duncan and O. V. Prezhdo, Annu. Rev. Phys. Chem. **58**, 143 (2007).